INTERFACE SCIENCE, 3, 107–118 (1995)

Mechanical Performance of Metal-Ceramic Interfaces Produced by Laser Processing

M. VAN DEN BURG AND J.TH.M. DE HOSSON
Department of Applied Physics, University of Groningen, Zernike Complex, Nijenborgh 4,9747AG Groningen, The Netherlands

Received March 11, 1994; Revised October 27, 1994

Abstract. This paper concentrates on the mechanical performance of various ceramic coatings of Cr_2O_3 on steel (SAF2205), as produced by CO_2 laser processing. The thickness of the coating that can be applied by laser coating is limited to about 200 μm setting a limit to the maximum strain energy release rate that can be measured in a 4 point flexure test before severe yielding occurs. In addition, a network of cracks with spacings of the order of 200 μm was always present in the laser applied coating preventing steady state crack growth along the interface.

It is concluded that a firmly bonded coating of Cr_2O_3 on steel could be produced by high power laser processing. The actual interface strength of a (Fe, Cr)-spinel applied to stainless steel by laser coating depends strongly on the composition of the substrate and coating materials. The energy release rate was extremely high and delamination occurred by fracture through the coating and partially along the interface, indicating that the interface strength is similar to or higher than the fracture strength of (Fe, Cr)-spinel.

Keywords: interfaces, metal-ceramic, laser, mechanical properties, coatings

1 Introduction

Several successful wear resisting materials consist of particles of a hard phase dispersed in a more ductile matrix. Using nowadays conventional techniques such as powder metallurgy techniques, the coatings remain frequently separated from the substrate by a sharp interface which is always a potential source of weakness. A different approach, followed in this paper, is to modify the surface layer by using a laser beam. Because of its high energy density, the laser beam is able to melt the metallic substrate and may even partly melt the ceramic powder. As a result, a solid bonding can be formed between the ceramic and the metal. However, as the physical properties between ceramic and metallic materials are much different, e.g. the thermal expansion coefficients and the crystallographic structures, cracks usually develop at the interface as well as inside the clad layer during the rapid solidification and cooling processes.

In previous publications [1, 2] we reported about the characteristic features of coating a duplex steel SAF 2205, stainless steel 304 and Fe-22 wt% Cr by bringing different powders into a laser beam. In fact a powder mixture of Cr_2O_3 and pure iron was brought into the laser beam in order to form a spinel structure inside the coating. Further, it turned out that it is possible to form a thick and homogeneous ceramic coating of Cr_2O_3 on steel by a proper selection of coating parameters such as scanning velocity, overlap and number of layers. A higher laser scan velocity may decrease the convection speed and prevents cracks in the coating induced by the convection. More than 50% overlap is needed in order to compensate for the lack of coating material in the center of the track being swept away by convection [1–4]. The work was concentrated on the stabilisation of high temperature distorted spinel phases due to the high quench rates involved as well as on the a quantitative crystallographic analysis of the resulting morphologies.

This paper concentrates on the actual performance of various coatings produced by laser processing. Performance of the laser applied coating is limited by its material property. However, it is quite rare that a material performance is determined by one single property. In particular the situations in which ceramic coatings are applied often demand upon a combination of corrosion and wear resistance, both of which are system properties rather than material properties as such. Unfortunately, standardized and specific experiments to

test such combinations of system properties are not well developed. This paper concentrates on the use of 3 and 4 point flexure tests.

The relevant physical quantities concern the critical elastic energy release rate G_c and the critical stress intensity factor K_c. The elastic energy release rate is obtained by equating the elastic energy released on crack growth to the energy required for the crack to propagate. For a plate of unit thickness the condition for crack growth becomes:

$$G = \frac{d}{da}(Q - U) \geq \frac{dW}{da} = R \qquad (1)$$

where U is the elastic energy contained in the plate, Q is the work performed by the external force and W is the energy for crack formation i.e. for brittle fracture the surface free energy. R is the crack resistance force. If G becomes larger than R the crack will propagate. As failure of the material occurs by growth of cracks the stress state at the crack tip is the most important parameter rather than the far field applied stress σ_{appl}. The stress σ_{yy} at the crack tip (on a crack plane $y = 0$) is characterized by the stress intensity factor K and failure under σ_f occurs when K reaches a critical value K_c. The critical energy release rate can be expressed for bimaterial interfaces as [5]:

$$G_c = \frac{2\left(\frac{1-\nu_1}{\mu_1} + \frac{1-\nu_2}{\mu_2}\right)}{4\cosh^2(\pi\varepsilon)} K\bar{K} \qquad (2)$$

Where μ represents the shear modulus, ν the corresponding Poisson's ratio's. ε is the so-called bimaterial constant and K is complex [6]. It is concluded that the critical stress intensity factor can be obtained from experimental values of the energy release rate.

2 Experimental

2.1 *Laser Coating of Cr_2O_3 on Steels*

A CW-CO_2-laser (Spectra Physics 820) is used for the laser coating process with the following laser parameters: 1.0 kW laser power, a spot size of 1.27 mm, a laser scan velocity of 20 mm/s and an overlap of 75% between the tracks. As coating powder Cr_2O_3, Cr_2O_3 containing Mn and Cr_2O_3 containing extra Cr and Mo are used. The Mn is added to investigate the influence of Mn on the lattice parameters of the (Fe, Cr)-spinel coating and on the interface between the substrate and the coating. Cr and Mo are added to manipulate the crystal structure of the melt pool in the austenitic stainless steels from fcc to bcc in order to change the thermal expansion coefficient of the substrate. The compositions of the coating powders are listed in Table 1.

Table 1. Compositions of various powders used.

Compositions (w%)	Cr_2O_3	Mn	Cr	Mo
1	100	—	—	—
2	92.5	7.5	—	—
3	75	25	—	—
4	66	—	20	14

As substrate the dual phase, with austenite and ferrite, SAF2205 steel is used of compositions: C(0.03), Si(1), Mn(2), Cr(22), Ni(5.5), Mo(3), bal Fe (in w%). Color etching and X-ray diffraction methods indicate that phases in the laser melted substrate are the same prior to and after laser treatment when Cr_2O_3 powder or Cr_2O_3 powder containing Mn is used. After coating with Cr_2O_3 powder containing extra Cr and Mo the melt pool in the substrate is completely transformed to bcc.

X-ray diffraction is used to identify the phases present in the laser coating. The peak positions of the $FeCr_2O_4$ and Cr_3O_4 phases [7] are used to calculate the lattice parameters of the (Fe, Cr)-spinel phases in the coating. Cross sectional TEM, SEM and SEM fractography as well as optical microscopy are applied to study the crack patterns and fracture surfaces in the laser applied coating. The composition of the different phases is analyzed using semi-quantitative EDS (energy dispersive X-ray spectroscopy).

2.2 *3- and 4-Point Flexure Tests: Determination of $G_{interface}$ and $K_{c(interface)}$*

The specimen used in the flexure experiments consists of a bimaterial beam (Fig. 1) with overall dimensions $40 \times 3 \times 3$ mm. The sides of the specimen are polished to facilitate optical observations during and after testing but the surfaces of the coatings are as received to prevent the formation of surface cracks due to grinding or polishing. The actual experiments are performed on duplex SAF2205 coated with a 200 μm plasma sprayed Cr_2O_3 coating and with a 100 μm laser applied (Fe, Cr)-spinel coating. Specimen with laser tracks parallel as well as perpendicular to the direction of loading are tested.

The flexure test consists of three steps, the first of which is making one or more Knoop indentations with the long diagonal of the indentation along the width

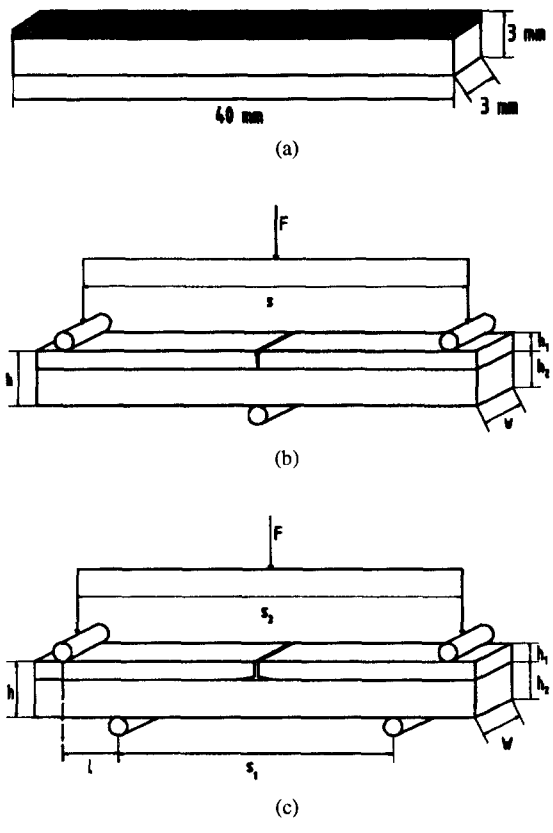

Fig. 1. (a) Bimaterial beam for testing interface properties. (b) Three-point flexure setup. (c) Four-point flexure setup.

of the specimen. A precrack is then made through the thickness of the coating along the line of the Knoop indentations by three point flexure. The objective of three-point flexure is to induce a symmetrical precrack along the bimaterial interface (Fig. 1b). The specimen is then loaded in four-point flexure (Fig. 1c) until delamination along the interface occurs. In systems where the coating makes up a substantial part of the total system, the load of delamination is determined by the load at which a load drop occurs. As the coating is only a small portion of the total system in the present case delamination is not accompanied by a significant load drop and interfacial delamination is monitored by acoustic emission.

The four-point flexure test is based on the storage of a well known amount of elastic energy on bending and a release of this elastic energy on fracture. The specimen rests on two rollers with two other rollers exerting a force on the specimen (Fig. 1c) resulting in a constant bending moment M in the region between the inner rollers: i.e. the same stress state is obtained throughout the region in between the inner rollers, making the experiment insensitive to the exact location of fracture. Consequently, the strain energy release rate upon delamination of the coating should exhibit steady state characteristics, at least when the interface crack length significantly exceeds the thickness of the coating. The steady state energy release rate G_{ss} can be deduced from the difference in the strain energy in the cracked and the uncracked beam. Since there is negligible strain energy in the beam above the crack, i.e. in the delaminated coating, the energy release rate is simply the difference in strain energy of the uncracked section and the section of the lower beam beneath the crack, i.e. of the substrate plus coating and the substrate respectively. Based on the description given by [8] for thin coatings, i.e. $h_1 \ll h_2 \approx h$, the strain energy release rate may be approximated by:

$$G_{ss} = \frac{18M^2(1-\nu_2^2)^2 E_1}{E_2^2(1-\nu_1^2)} \cdot \frac{h_1}{h^4}. \qquad (3)$$

As can be seen from Eq. (3) the strain energy release rate depends critically on the measured value of $h \approx h_2$. Interfacial crack propagation occurs when the strain energy release rate G_{ss} equals the critical energy release rate G_c of interfacial failure. The stress intensity factor K_c characterizing the bimaterial interface is obtained from Eq. (2).

3 Results

Cracks in the (Fe, Cr)-Spinel Ceramic Coating

Cracks in the ceramic coating are observed in the heat affected zone just outside the laser track (Fig. 2). In the (Fe, Cr)-spinel coatings on duplex steel SAF2205 it turned out that the cracks are oriented vertically in the coating and as a consequence do not cause delamination of the coating. However, complex delamination is observed when the coating thickness is larger than 200 μm. The vertical cracks run through the amorphous interdendritical phase and are deflected by the α-(Fe, Cr) particles. As the cracks run through the region of intergrowth between the (Fe, Cr)-spinel and the α-(Fe, Cr) particles the crack energy was not dissipated in the metallic particles. Consequently, the cracks run all the way through the coating and are blunted when they reach the substrate (Fig. 3). Here the crack is

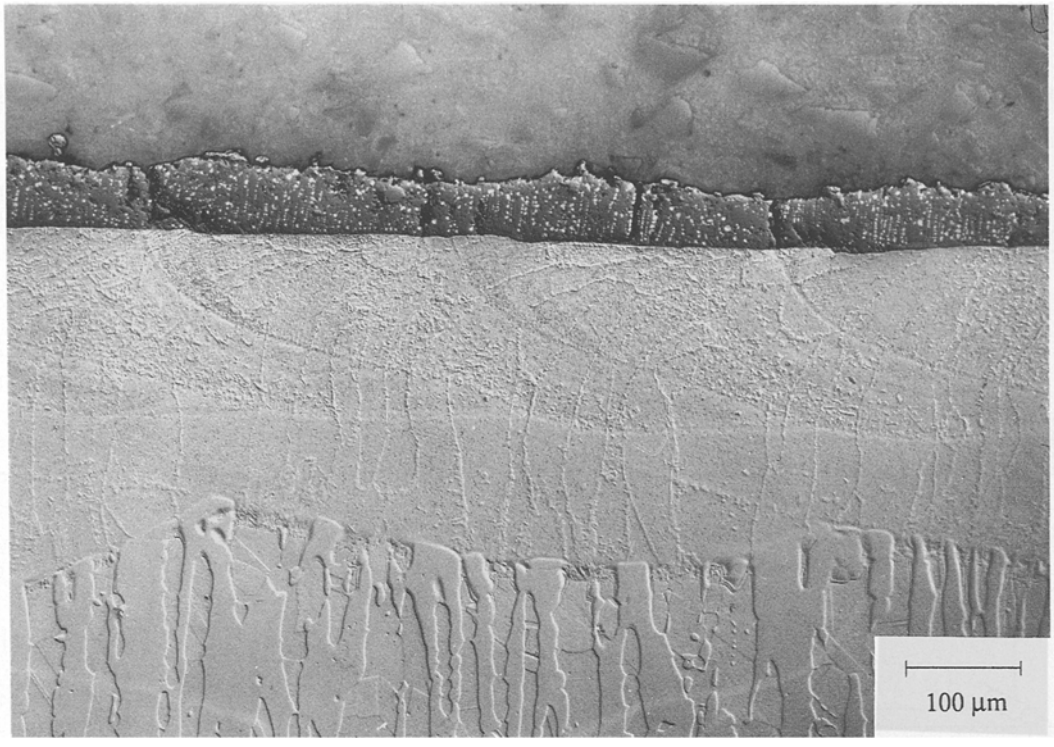

Fig. 2. Etched cross section of multiple overlapping laser tracks. Cracks parallel to the laser track are primarily in the heat affected zone.

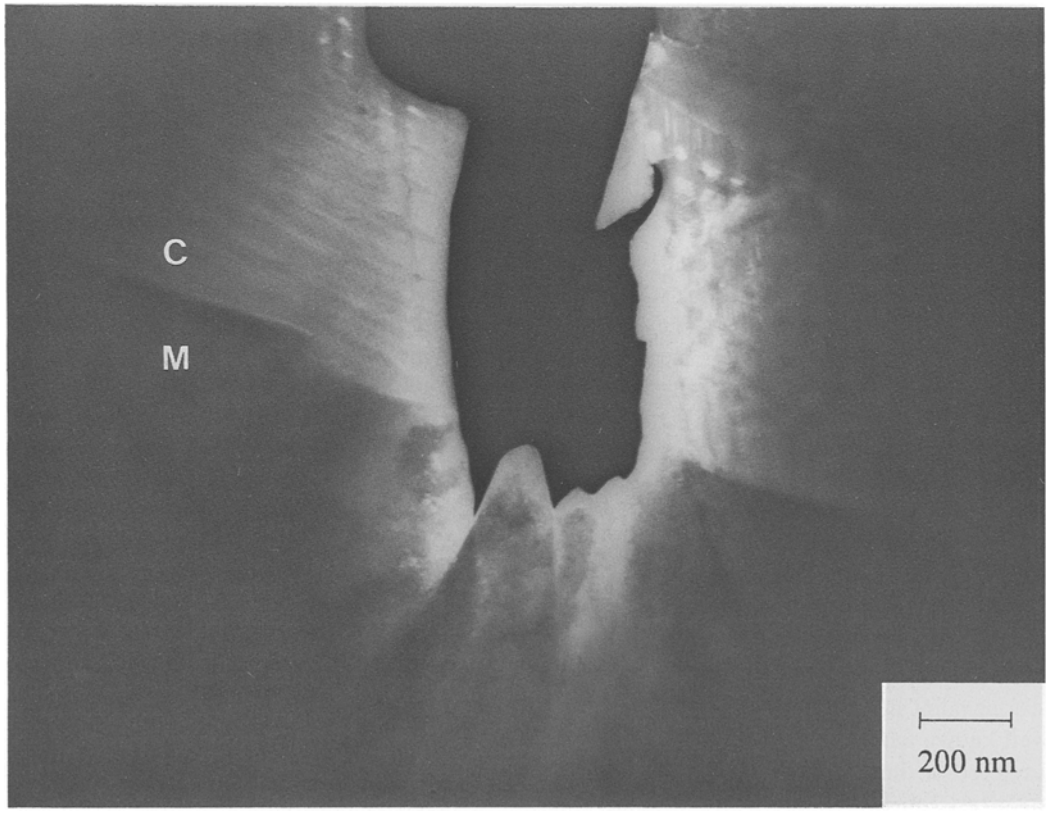

Fig. 3. TEM micrograph of (Fe, Cr)-spinel coating (C) on steel substrate (M) showing crack blunting in the steel.

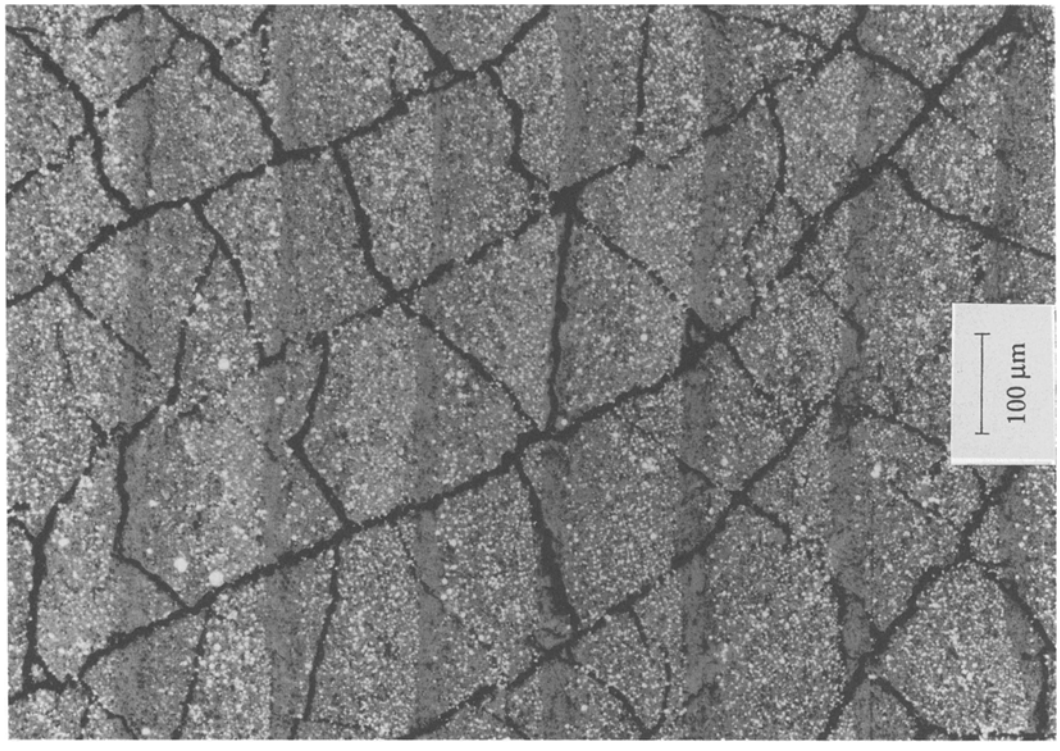

Fig. 4. Plane view of polished (Fe, Cr)-spinel surface showing two-dimensional network of cracks. Single laser tracks run downward and displacement of subsequent laser tracks is to the left.

opened by plastic deformation in the metal. Crack extension along the interface is not observed but crack branching in the ceramic coating is frequently observed in a region of 5 μm near the interface. A plane view on a polished section of the (Fe, Cr)-spinel coating shows a two-dimensional network of cracks (Fig. 4). One type of cracks is parallel to the laser track in the heat affected zone. The spacing between these cracks is caused by the transversal displacement of the laser beam. The other type of cracks makes an angle of 50°–70° with the direction of the laser beam (Fig. 4). When the transversal displacement of the laser beam is reversed the crack pattern is mirrored indicating a clear relationship with the geometry of the coating process and not with any irregularity of the Gaussian beam shape (TEM_{00} mode). These cracks are regularly spaced.

Effect of Mn on (Fe, Cr)-Spinel Coating

Experiments on SAF2205 and Fe_4Cr indicate that Mn plays a crucial role in preventing the decomposition from (Fe, Cr)-spinel to sesquioxide:

$$3M_3O_4 \rightarrow 4M_2O_3 + M.$$

When the specimen is not water cooled during laser treatment an important fraction of the coating on Fe_4Cr has decomposed to sesquioxide and metal. Only at the interface and the edge of the melt pool in the ceramic the coating remains (Fe, Cr)-spinel. The decomposition to sesquioxide is highly adverse because the decomposition is accompanied by a 5% volume reduction. As a consequence micro as well as macro cracks are running through the coating. When the specimens are water cooled the coating on both substrate materials remains (Fe, Cr)-spinel.

As the observed stabilization of the (Fe, Cr)-spinel occurs for Mn contents smaller than 1 a% experiments are performed to study the effect of larger Mn contents on the stabilization of the (Fe, Cr)-spinel and the bonding between the substrate and the coating. In the experiments specimens of SAF2205 are coated with Cr_2O_3 powder containing different fractions Mn. Plotting the composition of the different (Fe, Cr)-spinel coatings

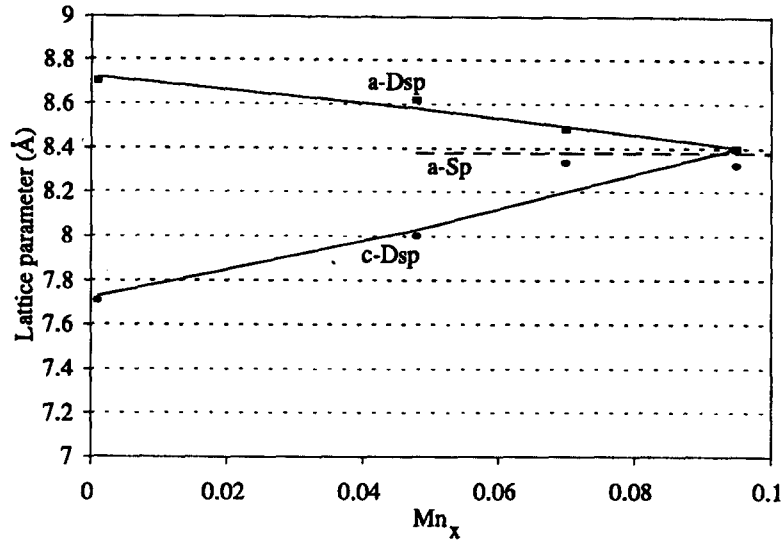

Fig. 5. Lattice parameters of tetragonally distorted (Fe, Cr)-spinel having composition $Fe_{0.3}Mn_xCr_{2.7-x}O_4$. Also indicated is the lattice parameter of cubic $FeCr_2O_4$.

versus the lattice parameters as calculated from X-ray diffractions data results in Fig. 5. The lattice parameters are indexed in the cubic spinel system to facilitate observation of the tetragonality of the system. It is clear from Fig. 5 that the (Fe, Cr)-spinel becomes more cubic upon adding extra Mn. The coatings on SAF2205 exhibits a similar behavior of composition versus lattice parameters indicating that elements other than Fe, Cr and Mn play no important role in the formation of (Fe, Cr)-spinel coatings. The results of the flexure experiments refer to the Cr_2O_3 coatings onto SAF2205, without extra addition of Mn.

Flexure Tests

The thickness of the coating that can be applied by laser coating is limited to about 200 μm setting a limit to the maximum strain energy release rate that can be measured before serve yielding occurs. Furthermore, a network of cracks with spacings of the order of 200 μm is always present in the laser applied coating. When the specimens having laser applied Cr_2O_3 coatings are set up in 4-point flexure two modes of failure may occur. First of all delamination along the interface is possible resulting in a value for the critical energy release rate and the stress intensity factor. The value obtained is a minimum value because of the large tensile stresses present in laser treated materials. In order to obtain an actual value of the critical energy release rate the strain energy present after laser treatment should be superimposed onto the strain energy stored during bending. The stress state after the laser treatment is however inhomogeneous due to the localized character of the laser melting. When the interface is very strong the cracks through the coating will not extend along the interface but will blunt by plastic deformation of the substrate.

In the present case failure occurs by crack blunting in the substrate as can be seen from Fig. 6. In Fig. 6 the edge of the specimen is polished before 4-point flexure and the size of the deformed volume can be observed by the plane stress type of necking. Only in some cases delamination occurs after work hardening of the substrate (Fig. 7). Assuming that the plastic deformation only occurs in a small volume near a crack through the coating the amount of energy stored, and thus a minimum value for the critical energy release rate, can still be obtained from the maximum load. Observations indicate that the critical strain energy release rate and stress intensity factor are at least larger than:

$$G_{ss}^{\min} = 270\ [\mathrm{J/m^2}]$$
$$\left|K_c^{\min}\right| = 8.5\ [\mathrm{MPa}\sqrt{\mathrm{m}}]$$

The value of the critical energy release rate has to be considered as a lower bound value.

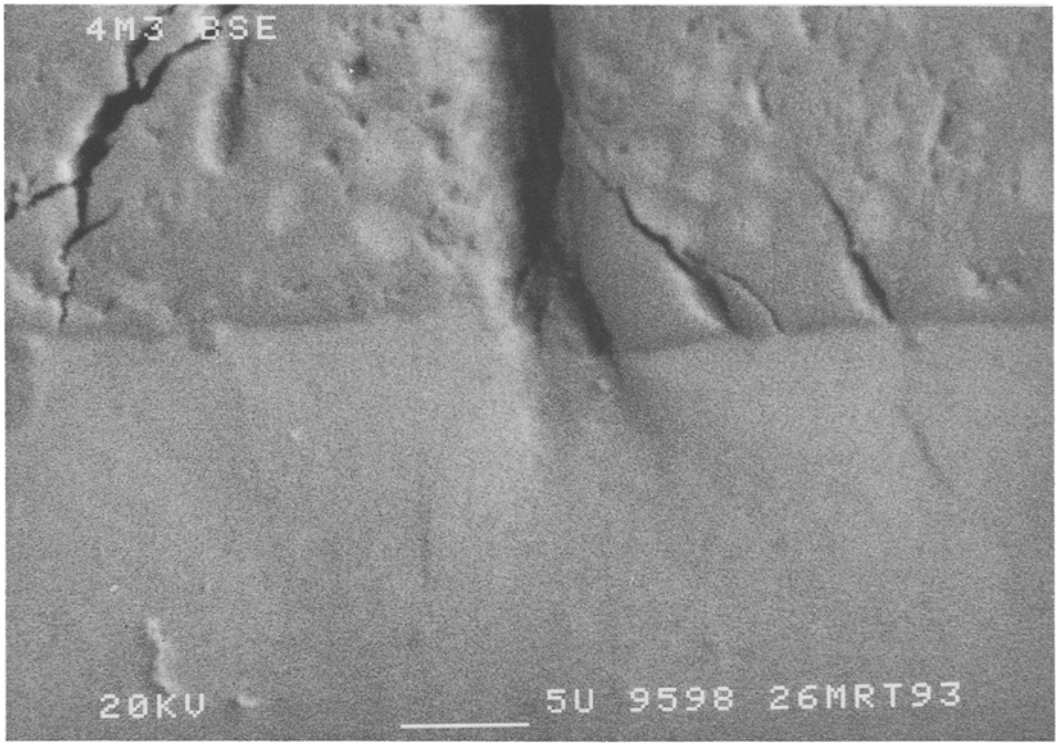

Fig. 6. Crack blunting in the steel substrate during four-point flexure. Necking of the polished substrate shows the extend of plastic deformation in the substrate.

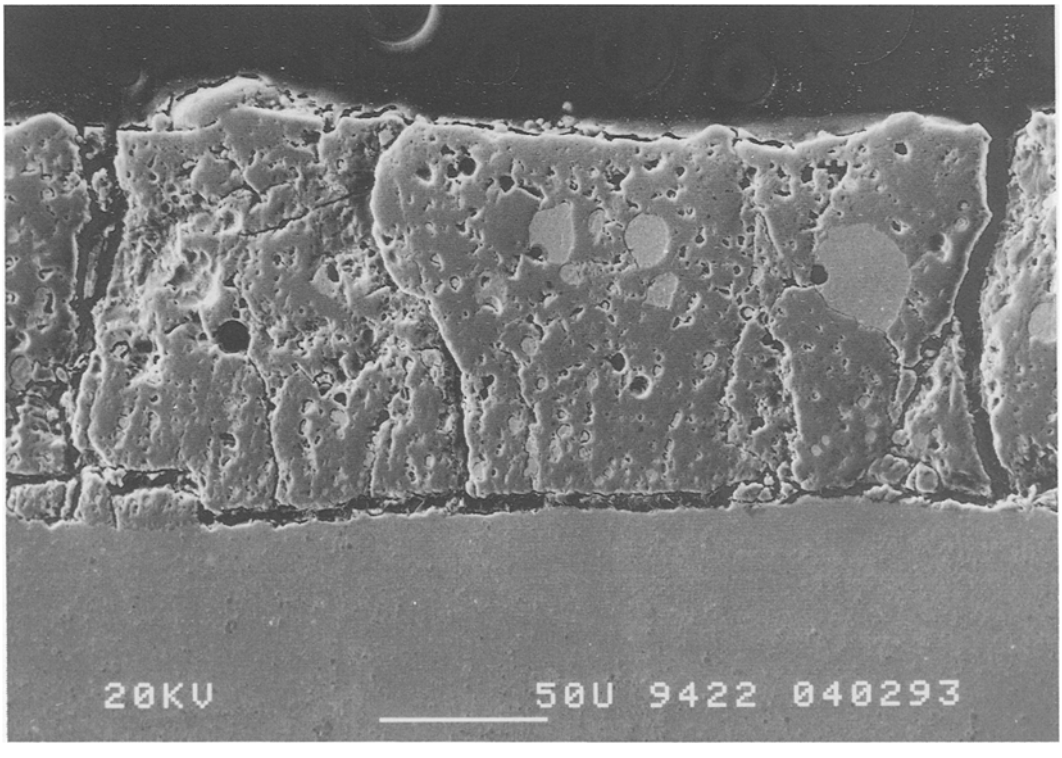

Fig. 7. Crack propagation along the interface after work hardening of the substrate.

4 Discussion

Results in the literature on the laser application of ceramic coatings are scarcely available indicating that laser coating with ceramic materials is rather difficult. The problem is caused by the inhomogeneous heating and subsequent cooling during laser treatment which result in considerable cooling strains. In metals these strains are accommodated by plasticity, likewise in ceramics at high temperatures ($T > 2/3\ T_m$). At low temperatures strain results in fracture of the ceramic. When metals are coated with ceramic material fracture may take place either through the coating or along the interface depending on the bond strength of the interface and the difference in thermal expansion coefficient. However, a systematic investigation of interfaces is hampered by the detrimental effect of impurities on the interfacial properties, especially in the laser coating process where the solidification of the metallic melt pool towards the interface pushes impurities towards the interface. Impurities in the ceramic coating are less problematic because the solidification of the coating starts from the interface.

The thermal loading by the laser beam causes stresses being build up. Without melting or yielding all thermal strains will be accommodated elastically, i.e. disappear when returning to the starting temperature. Melting or yielding is necessary in order to attain a residual stress state. Because the cooling during laser treatment starts from the bottom to the surface of the specimen the residual stress state near the surface of the specimen, i.e. the ceramic coating, will be of tensile character. The residual stress adds up with the mechanically applied stresses causing failure at relatively low levels of applied stress. To study the formation of cracks during and after laser treatment we have scrutinized the temperature field near the laser melt pool to obtain the stress during and after laser treatment based on the work by Cline and Anthony [9]. The temperature field is calculated of a Gaussian beam sweeping over the surface of a material. By taken derivatives with respect to x and y the thermal gradients $\frac{\partial T}{\partial x}$, $\frac{\partial T}{\partial y}$ and the absolute value of the total gradient is obtained. Numerical values are displayed in Fig. 8. It is clearly visible that, although the melt pool is only slightly elongated in the x-direction the maximum thermal gradients are on both sides of the melt pool. The temperature field and thermal gradients are also evaluated for the laser melt pool in material having a ten times lower thermal conduction coefficient, i.e. for a melt pool in (Fe, Cr)-spinel. Then the melt pool is very elongated in the x-direction and heat conduction is almost completely in the y- and z-direction. Although we did not solve the three dimensional temperature field numerically for a bimaterial we may extrapolate the data from the two singular cases of steel and (Fe, Cr)-spinel using the diffusion equation together with the fact that the temperature field has to be continuous across the interface. This implies that the thermal gradients parallel to the interface, i.e. in the x- and y-direction, are equal on both sides of the interface ($z = 0$ on the interface):

$$\left(\frac{\partial T}{\partial x}\right)^{\text{met}}_{x,y,0} = \left(\frac{\partial T}{\partial x}\right)^{\text{cer}}_{x,y} \tag{4a}$$

$$\left(\frac{\partial T}{\partial y}\right)^{\text{met}}_{x,y,0} = \left(\frac{\partial T}{\partial y}\right)^{\text{cer}}_{x,y} \tag{4b}$$

and

$$k_{\text{met}}\left(\frac{\partial T}{\partial z}\right)^{\text{met}}_{x,y,0} = k_{\text{cer}}\left(\frac{\partial T}{\partial z}\right)^{\text{cer}}_{x,y,0}$$

$$\Rightarrow \left(\frac{\partial T}{\partial z}\right)^{\text{cer}}_{x,y,0} \approx 10\left(\frac{\partial T}{\partial z}\right) \tag{4c}$$

using the fact the heat flux is continuous over the interface. Observations of the equi-temperature lines on the interface perpendicular to the direction of the laser beam, i.e. in the y-direction, indicate that for the (Fe, Cr)-spinel coating on steel:

$$\left(\frac{\partial T}{\partial z}\right)^{\text{met}}_{x,y,0} \approx 0.26\left(\frac{\partial T}{\partial y}\right)^{\text{met}}_{x,y,0} \tag{5}$$

$$\left(\frac{\partial T}{\partial z}\right)^{\text{cer}}_{x,y,0} \approx 2.6\left(\frac{\partial T}{\partial y}\right)^{\text{cer}}_{x,y,0} = 2.6\left(\frac{\partial T}{\partial y}\right)^{\text{met}}_{x,y,0} \tag{6}$$

Equation (5) shows that, in the metal, the thermal gradient in the z-direction is only one quarter of the gradient in the y-direction validating the use of the temperature field calculated for a single phase steel having a zero thermal gradient in the z-direction on the surface. Equation (6) indicates that the large temperature gradient in the y-direction is accompanied by a more than twice as large thermal gradient in the z-direction in the ceramic coating. From the thermal gradient in the y-direction of $1.8 \cdot 10^6$°C/m in steel a thermal gradient in the z-direction of $4.7 \cdot 10^6$°C/m is estimated in the (Fe, Cr)-spinel coating. As these large thermal gradients occur at temperatures near the melting point they are accompanied by low stress levels. However, during cooling the temperature difference results in the build-up of residual stresses. Because, in the region of

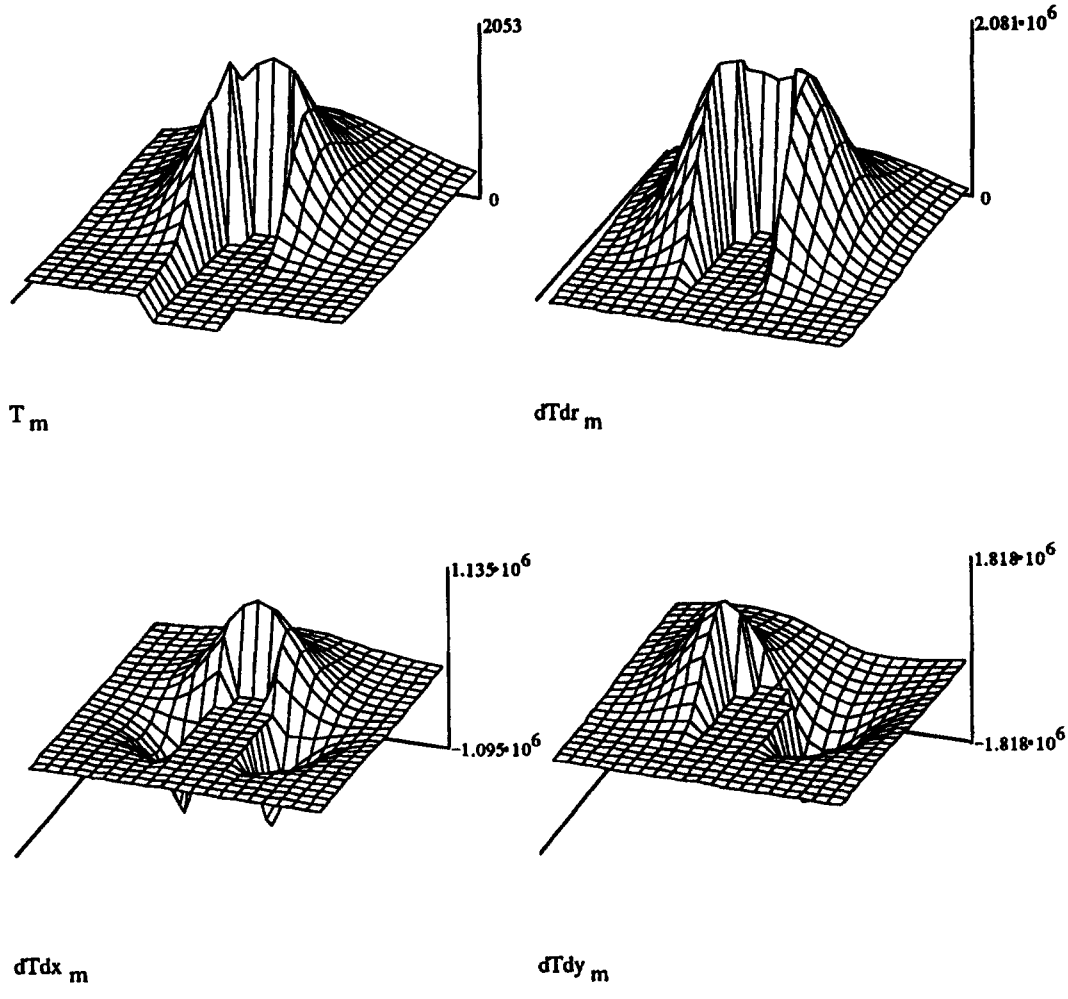

Fig. 8. Numerical values of temperature field, thermal gradient and thermal gradient in x- and y-direction. Laser beam movement is in the $+x$-direction.

interest, the coating cools from the interface towards the top of the coating the stress is of tensile character in the top of the coating, i.e. a bending moment is set up in the coating that may cause delamination of the ceramic coating.

The residual stress state can be estimated from the solution of a bending plate on an elastic foundation of which the solution is known. When bending is restricted by the substrate, i.e. edges are clamped and delamination does not occur, the stress in the top of the coating is given by:

$$\sigma_{yy}(z) = \frac{\alpha_1 E_1 \frac{\partial T}{\partial z}}{(1-\nu_1)} \cdot z, \tag{7}$$

where index 1 refers to the properties of the coating. The temperature field at a depth z upon cooling can be approximated by:

$$T(z,t) = T_0 + (T_r - T_0)\mathrm{erfc}(z/2\sqrt{t\alpha_D}), \tag{8}$$

where α_D is the thermal diffusivity ($6.4 \cdot 10^{-7}$ m^{2}s^{-1} in Cr_2O_3). Clearly there exists a stress distribution over the thickness of the coating which sets up a bending moment in the coating which can be approximately written as:

$$M_1 = \frac{\alpha_1 E_1 \frac{\partial T}{\partial z}}{12(1-\nu_1)} \cdot h_1^3. \tag{9}$$

Using Eqs. (7) and (8) the bending moment is found to be 14.2 Nm/m for a coating thickness of 200 μm. which is close to the outcome of Eq. (9), namely 13.7 Nm/m.

When the coating does not delaminate edge moments have to be applied to prevent bending. These

edge moments are effectively produced by stress components in the z-direction over the interface. The stress σ_{zz} at the edge of a bending plate is given by Hetenyi [10] and the maximum tensile stress is given by:

$$\sigma_{zz}^{\max} = 2 \cdot \frac{\alpha_1 E_1 \frac{\partial T}{\partial z}}{12(1-\nu_1)} \cdot \sqrt{\frac{3k_2}{E_1}} \cdot h_1^{1\frac{1}{2}}, \qquad (10)$$

where k_2 is the modulus of deflection of the substrate ($E_1/k_2 = 6.6 \cdot 10^{-5}$). In the laser coating process several laser tracks have to be applied before the coating reaches its final thickness, i.e. its final stress state. Realizing that an edge moment, and thus a stress σ_{zz}, is only generated at a free edge one crack through the thickness of the coating is always present. After the first crack parallel to the laser track two things may happen. First, delamination may start from the free edge and grow to the last laser track applied where the coating becomes thinner and crack propagation will stop. When delamination occurs the stress σ_{yy} is removed by bending of the coating so on further cracking through the thickness of the coating will occur. Another possibility is that the stress σ_{zz} at the free edge is not large enough to cause delamination. Then the stress σ_{yy} is locally reduced due to crack opening but is unchanged in the rest of the coating. As a result cracks more or less regularly spaced will appear through the thickness of the coating.

The process of delamination versus perpendicular fracture is determined by the relative strength of the ceramic and the interface and by the thickness of the coating. As the stress σ_{yy}, causing fracture through the coating, scales with h_1 and σ_{zz}, causing delamination, scales with $h_1^{1.5}$ the coating can always be made thick enough so that delamination will occur. Ultimately, when the interface is very strong, delamination may occur by fracture through the ceramic parallel to the interface, instead of along the metal-ceramic interface, and both fracture processes are governed by the strength of the ceramic σ_f^c, being of the order of 1 GPa. If this is the case the fracture process, i.e. delamination vs. perpendicular fracture, is solely determined by the coating thickness and the critical coating thickness is determined by the elastic properties of the coating and the substrate. Whether or not fracture will occur is of course related to the thermal gradient in the coating. Assuming that the thermal gradient is large enough for fracture to occur delamination is the governing process if:

$$h_1 > \frac{3E_1}{k_2}. \qquad (11)$$

Using the experimental maximum coating thickness of 200 μm for the (Fe, Cr)-spinel coating on SAF2205, where delamination is mainly through the ceramic, the critical bending moment M_{1c} is calculated to be 14.2 Nm/m. From the calculated bending moment in the ceramic coating the critical energy release rate G_{ss} of delamination can be calculated:

$$G_c = \frac{M_{1c}^2(1-\nu_1)^2}{2E_1} \cdot \frac{12}{h_1^3} = 320\ [\mathrm{J/m^2}] \qquad (12)$$

The question is whether the gradient of the residual stress distribution in a coating of a thickness of 200 μm would predict delamination. For this purpose, the energy release rate of Eq. (12) is written in the usual form, i.e. in terms of the stress intensity factor K. The problem of delamination due to edge loads and moments was solved by [11, 12]. However, usually there is a significant amount of mode II component involved whereas we like to focus here on a critical thickness h_c corresponding responding to a pure mode I trajectory. The problem involves a non-linear algebraic equation, the solution of which we display in Fig. 9 as a function of $\kappa = h_c/\sqrt{\alpha_D t}$. The mode I stress intensity factor is found to be $K_{Ic} = 0.189\sigma\sqrt{h_c}$, forcing K_{IIc} equal to zero. From a critical energy release rate (Eq. 2) expressed in terms of K_{Ic} and the calculated value of 320 J/m (Eq. 12) follows for $h_c = 200$ μm a stress level of 1.3 GPa. Indeed the latter is about the fracture stress of a ceramic material. Therefore we may expect that a thick coating of 200 μm will delaminate by fracture through the ceramic material parallel to the interface, instead of along the metal-ceramic interface. The latter is in accordance to experimental observations. It should be noted that the crack path

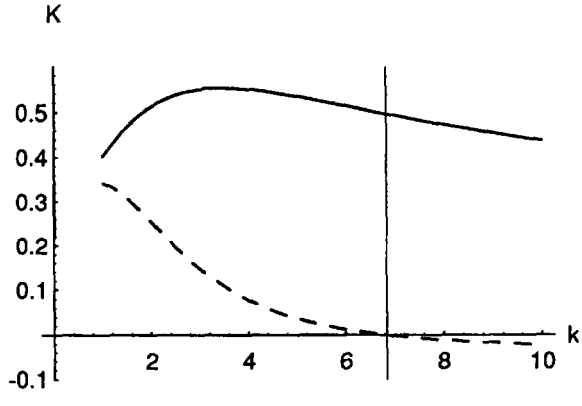

Fig. 9. Stress intensity factors as a function of a function of $\kappa = h_c/\sqrt{\alpha_D t}$ (Solid line K_I, dashed line K_{II}).

will deviate from a planar delamination if K_{II} is not equal to zero.

If delamination does not occur the stress σ_{yy} is reduced due to crack opening. The wavelength of the stress reduction is related to the extend of the stress field across the interface and scales with $h_1^{3/4}$. As the maximum value of the stress σ_{yy} scales with h_1, the distance over which the fracture stress σ_f^c is reached scales with $h_1^{1/4}$ indicating that the crack spacing is only weakly dependent on the thickness of the coating. For a coating of 100 μm the extension of the stress field over the interface is about 200 μm indicating a crack spacing of the same size. This is in agreement with experimentally observed crack spacings. However, these crack spacings also scale with the transversal displacement of the laser beam. This is partially because the thermal gradient peak in the metal causes an extended gradient peak in the ceramic. In this way a region of large stress parallel to the laser track is developed where fracture takes place preferentially. This effect is augmented by the fact that the ceramic coating is somewhat thicker at the edge of the metallic melt pool, i.e. at the same place where the gradients are largest. It can thus be concluded that the crack spacing is more strongly related to the stress peaks in the coating, i.e. to the transversal displacement of the laser beam, rather than to areas where the stress is reduced due to a prior crack.

A similar explanation can be given for the stress development in the x-direction, i.e. in the direction of movement of the laser beam. Although the thermal gradients in the z-direction in the coating can be very large due to the thermal gradients in the x-direction delamination in the x-direction is never observed because the coating thickness is always much smaller near the middle of the last laser track that is applied. However, the stress in the x-direction scales with the thermal gradient in the z-direction near the middle of the laser track so that fracture through the coating, more or less perpendicular to the direction of movement of the laser beam is always observed. For all other cases where the heat flow is not purely in the x- or y-direction the stress in the coating is determined by the total magnitude of the thermal gradient. Because of the low thermal conduction coefficient the flow of heat from the coating is however mainly in the y-direction making delamination in the y-direction of the most significant process.

Another point to consider is the stress development during laser treatment: influence of thermal expansion difference $\Delta\alpha$. A difference in thermal expansion coefficient between the coating and the substrate material can result in normal and in shear stresses. In the present case of coating ceramic material on steel using a high power laser shear stresses will be set up due to the asymmetry of the process. As the laser track is restricted by the surrounding material a tensile stress will be present in both materials near the interface but, as no macroscopic shrinkage can occur the stress is not transmitted over the interface. However, because during laser treatment the material closer to the center of the laser track is at a higher temperature, yielding will cause a net flow of material in the outward direction. The magnitude of the net displacement of material will scale with the thermal expansion coefficient α of the corresponding material.

Four-point flexure appeared to be an appropriate method to test the interfacial properties of bimaterials. However, there are also a new limitation, one of which is the maximum energy release rate that can be measured when investigating thin coatings on ductile substrates. For a 100 μm (Fe, Cr)-spinel coating on duplex the maximum energy release rate is of the order of 160 J/m^2 for a specimen thickness of 3 mm. The value of 270 J/m^2 as obtained experimentally involves some substrate yielding making work hardening of the substrate and interface sliding possible. For a reliable measurement of the critical energy release rate this should be prevented but it can be used to obtain an indication of the quality of the interface. The elastic energy stored in a 100 μm thick coating due to the laser treatment is only 37 J/m^2 so in order to get delamination during 4-point flexure about 280 J/m^2 should be applied to the coating by bending. However, yielding of the substrate limits the elastic energy stored in the coating to 160 J/m^2 making delamination of a 100 μm (Fe, Cr)-spinel coating by 4-point flexure impossible.

5 Conclusion

It is concluded that a firmly bonded coating of Cr_2O_3 on steel could be produced by high power laser processing. The actual interface strength of a (Fe, Cr)-spinel applied to stainless steel by laser coating depends strongly on the composition of the substrate and coating materials. The strength of bimaterial interfaces was tested by 4-point flexure. The energy release rate was extremely high and delamination occurred by fracture through the coating the partially along the interface, indicating that the interface strength is similar to or higher than the fracture strength of (Fe, Cr)-spinel.

Acknowledgments

This work is part of the research of IOP-metals (C89 427 RG XX) The Hague, The Netherlands Foundation for Fundamental Research on Matter (FOM-Utrecht) and has been made possible by financial support from the Netherlands Organization for Research (The Hague).

References

1. X.B. Zhou and J.Th.M. De Hosson, Acta Metall. Mater. **39**, 2267 (1991).
2. J.Th.M. De Hosson, X.B. Zhou, and M. van den Burg, Acta Metall. Mater. **40**, S139 (1992).
3. M. van den Burg and J.Th.M. De Hosson, J. Mat. Res. **9**, 142 (1994).
4. M. van den Burg and J.Th.M. De Hosson, Acta Metall. Mater. **41**, 2557 (1993).
5. M.F. Kanninen and Popelar, Advanced Fracture Mechanics, Oxford University Press, New York (1985).
6. J.R. Rice, J. Appl. Mech. **55**, 98 (1988).
7. D.C. Hilty, W.D. Forgeng, and R.L. Folkman, Metall. Trans. **203**, 253 (1955).
8. J.R. Rice, *Fracture: An Advanced Treatise*, edited by H. Liebowitz **22**, 191 (1968).
9. H.E. Cline and T.R. Anthony, J. Appl. Phys. **48**, 3895 (1977).
10. M. Hetenyi, Beams on Elastic Foundations, The University of Michigan Press (1946).
11. J.W. Hutchinson, Adv. Applied Mech. **29**, 63 (1993).
12. M.D. Thouless, A.G. Evans, M.F. Ashby, and J.W. Hutchinson, Acta Metall. **35**, 1333 (1987).